



Review of Incoherent Digital Holography: Applications to Multidimensional Incoherent Digital Holographic Microscopy and Palm-Sized Digital Holographic Recorder – Holosensor

Tatsuki Tahara*

Applied Electromagnetic Research Center, Radio Research Institute, National Institute of Information and Communications Technology, Koganei, Japan

OPEN ACCESS

Edited by:

Peter Wai Ming Tsang,
City University of Hong Kong, Hong
Kong SAR, China

Reviewed by:

Jung-Ping Liu,
Feng Chia University, Taiwan
Myung Kim,
University of South Florida,
United States

*Correspondence:

Tatsuki Tahara
tahara@nict.go.jp

Specialty section:

This article was submitted to
Optical Information Processing and
Holography,
a section of the journal
Frontiers in Photonics

Received: 05 December 2021

Accepted: 27 December 2021

Published: 01 February 2022

Citation:

Tahara T (2022) Review of Incoherent
Digital Holography: Applications to
Multidimensional Incoherent Digital
Holographic Microscopy and Palm-
Sized Digital
Holographic Recorder – Holosensor.
Front. Photonics 2:829139.
doi: 10.3389/fphot.2021.829139

We review advancements in incoherent digital holography (IDH) with an image sensor and its applications to multidimensional microscopy and a palm-sized hologram recorder termed “holosensor”. There are two types of representative IDH technique: IDH with a structured illumination and a single photodetector termed optical scanning holography and self-interference IDH. The latter IDH is a technique to obtain an incoherent digital hologram by modulating an incoherent light wave between an object and an image sensor. Multidimensional information such as three-dimensional space and wavelengths is simultaneously recorded without changing optical filters by introducing interferometric techniques invented in laser holography. Applications to high-speed color-multiplexed holographic fluorescence microscopy, single-shot incoherent full-color holographic microscopy with white light, and a palm-sized multidimensional incoherent hologram recorder have been developed using multidimensional IDH systems. Schematics and experimental results obtained using IDH techniques, incoherent holographic microscopy systems, and compact IDH systems are introduced.

Keywords: incoherent digital holography, digital holography, digital holographic microscopy, color holography, three-dimensional microscopy, holographic fluorescence microscopy, computational coherent superposition, holosensor

1 INTRODUCTION

Multidimensional imaging is one of the most actively researched themes in both science and industry. Multidimensional information, such as three-dimensional (3D), wavelength, and polarization images, has been applied to observe realistic scenes of remote locations, microscopic and nanoscopic fields of view, and invisible images at infrared wavelength bands. 3D information is important, particularly when a person and a machine perceive and observe 3D structures of samples and scenes. Color and polarization information is useful for accurately identifying and distinguishing objects. Image sensors at various wavelength bands and polarization-imaging cameras have been developed, and multimodal imaging with such sensors has been performed to date. Multiple image

sensors and various optical filters are generally used to record multidimensional information. However, advanced optical techniques have been desired to make it possible to realize a compact multidimensional imaging system.

Incoherent digital holography (IDH) is an optical technique of 3D imaging with a single sensor. 3D information of a light wave is recorded using light interference. A hologram is digitally recorded even for a spatially incoherent light wave. The 3D image of a light wave is reconstructed from the recorded hologram using a computer. Multiple image sensors are not required for 3D imaging. The invention of IDH originated from the proposal of incoherent holography (Lohmann, 1965). Lohmann proposed several optical implementations including self-interference and self-reference holography to obtain a hologram of spatially incoherent light and demonstrated holographic imaging with an implementation (Lohmann and Bryngdahl, 1968). After that, Poon *et al.* invented IDH with a single photodetector termed optical scanning holography (OSH) (Poon and Korpel, 1979; Poon, 1985). OSH is a single-pixel DH technique with a structured illumination. By exploiting point-spread-function (PSF) engineering of illumination light and a temporal heterodyne technique, one can encode 3D information of fluorescence light as time-series intensity values. The 3D information of fluorescence light is recorded by a single photodetector. Holographic fluorescence microscopy was initially invented with OSH in 1997 (Schilling *et al.*, 1997), and IDH imaging was performed for fluorescence light. On the other hand, research on incoherent holography with a 2D recording material has been continued. Sirat and Psaltis proposed and experimentally demonstrated an incoherent holography system equipped with a birefringent material and polarizers to generate interference light, and they termed the technique conoscopic holography (CH) (Sirat and Psaltis, 1985). CH has been implemented with a unique phase-shifting interferometry (PSI) system employing a liquid crystal phase modulator and a rotational amplitude mask (Mugnier and Sirat, 1992; Mugnier *et al.*, 1993; Mugnier, 1995). Such a single-path polarimetric interferometer contributes to the construction of today's compact IDH system. Then, Yoshimori proposed an IDH technique to conduct hyperspectral 3D imaging of natural light based on Fourier spectroscopy (Yoshimori, 2001). After that, Rosen and Brooker proposed an IDH technique that adopts a phase-only spatial light modulator (SLM) both to construct a self-interference IDH system and to conduct PSI, and the technique was termed Fresnel incoherent correlation holography (FINCH) (Rosen and Brooker, 2007). An incoherent digital hologram is obtained without the use of a structured illumination, and incoherent holographic imaging is conducted with several exposures. Application to holographic fluorescence microscopy with an image sensor was demonstrated (Rosen and Brooker, 2008), and then PSF improvement in incoherent imaging by FINCH was achieved (Rosen *et al.*, 2011). As another application of IDH, Kim performed high-quality incoherent holographic imaging, including full-color 3D imaging of an outdoor scene illuminated by sunlight (Kim, 2013; Clark and Kim, 2015). From these research achievements, IDH can be applied to the holographic imaging of various light waves.

Progress on IDH comes from exploiting optical devices and state-of-the-art holographic techniques that are invented in incoherent and laser holography. An image sensor with a wide dynamic range and low noise enables us to record low-visibility incoherent holograms. The combination of PSI (Bruning *et al.*, 1974; Yamaguchi and Zhang, 1997) with a phase-only SLM or a highly accurate piezo actuator improves image quality because undesired-order diffraction images are removed by digital signal processing based on interferometry. Further advancement of IDH is expected by adopting a laser holography technique to IDH.

Research on laser DH has been continuously conducted, and techniques invented in laser DH have been actively adopted to IDH in the last 5 years: single-shot IDH (Tahara *et al.*, 2017a; Nobukawa *et al.*, 2018; Choi *et al.*, 2019; Tahara *et al.*, 2020a; Liang *et al.*, 2020) with single-shot phase-shifting (SSPS) (Zhu and Ueda, 2003; Awatsuji *et al.*, 2004; Millerd *et al.*, 2004), single-path multiwavelength-multiplexed IDH (Tahara *et al.*, 2019; Tahara *et al.*, 2020b; Hara *et al.*, 2020; Tahara *et al.*, 2021a; Tahara *et al.*, 2021b) based on computational coherent superposition (CCS) (Tahara *et al.*, 2015a; Tahara *et al.*, 2015b; Tahara *et al.*, 2017b; Tahara *et al.*, 2018a), and single-shot multicolor IDH techniques (Tahara *et al.*, 2020c; Tahara *et al.*, 2021). Applications of IDH, such as multidimensional holographic microscopy with incoherent light and the palm-sized hologram recorder “holosensor” (Tahara, 2021; Tahara and Oi, 2021; Tahara *et al.*, 2021; Tahara *et al.*, 2021c), are proposed using the developed IDH techniques. In this review, IDH techniques are explained and applications to multidimensional microscopy and holosensor are introduced.

2 INCOHERENT DIGITAL HOLOGRAPHY

IDH is implemented by PSF engineering of an illumination light wave or an object wave. OSH is for the former and other proposed IDH techniques are for the latter. **Figure 1** illustrates examples of IDH with a structure illumination, which is termed OSH, and IDH with self-interference light. **Figure 1A** is a schematic of OSH. A Gabor zone plate (GZP) pattern illuminates an object. The generation of the GZP pattern means PSF engineering of illumination light in 3D space. The GZP pattern moves along an X-Y plane. A single-pixel photo detector records time-sequence intensity data and this data contains 3D information of the object. A 3D image without the zeroth-order diffraction wave and the conjugate image is reconstructed using a temporal heterodyne technique. This technique is categorized as single-pixel DH and spatially incoherent DH. A book and comprehensive review articles for OSH have been written by experts to date, and these will help readers understand DH techniques with a single photodetector (Poon, 2007; Ting-Chung Poon *et al.*, 1996; Poon, 2009; Liu *et al.*, 2018). **Figures 1B,C** are schematics of self-interference IDH using rotational and radial shears, respectively. A shear is utilized to generate self-interference in many IDH techniques. Yoshimori and co-workers have proposed and experimentally demonstrated hyperspectral 3D imaging with commonly used light by constructing a Michelson-type IDH system utilizing a

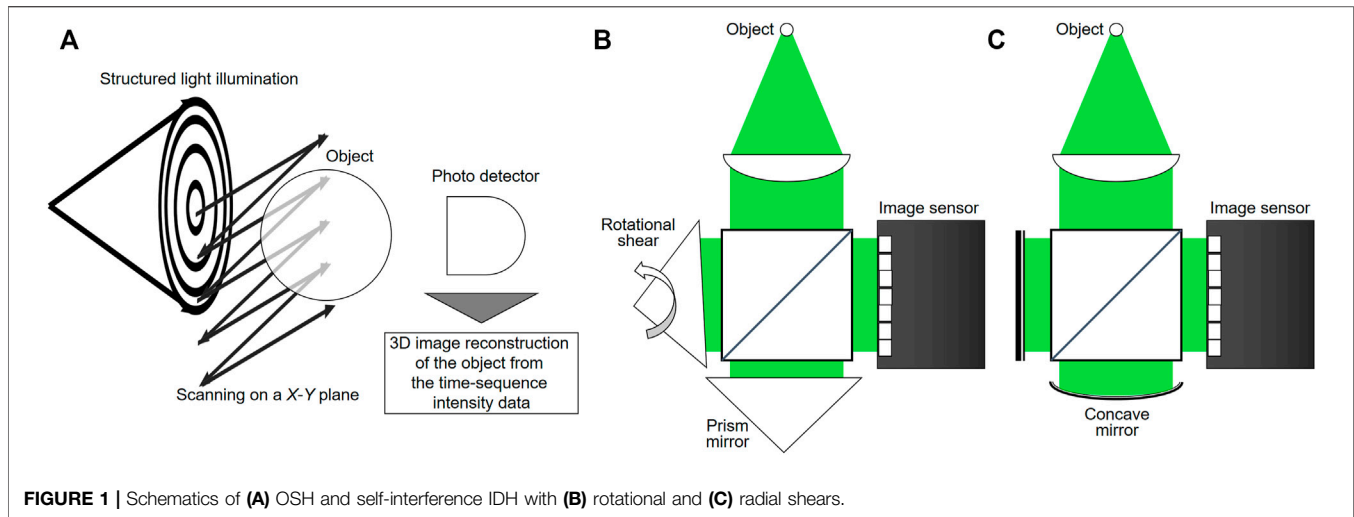


FIGURE 1 | Schematics of (A) OSH and self-interference IDH with (B) rotational and (C) radial shears.

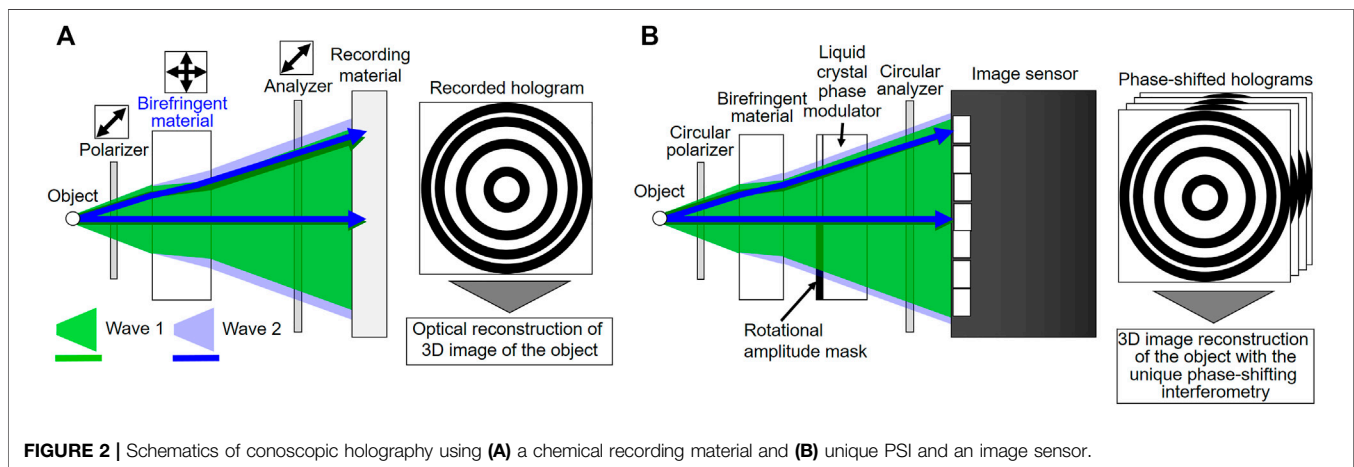


FIGURE 2 | Schematics of conoscopic holography using (A) a chemical recording material and (B) unique PSI and an image sensor.

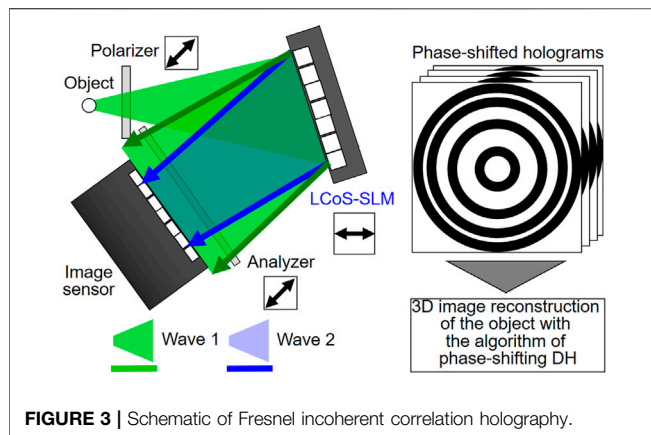
rotational shear shown in **Figure 1B** (Yoshimori, 2001; Teeranutranoont and Yoshimori, 2013). Kim and co-workers and other researchers have proposed a Michelson-type self-interference IDH system using a concave mirror to generate a radial shear shown in **Figure 1C** (Kim, 2012; Hong and Kim, 2013; Kim, 2013). Kim has demonstrated full-color 3D imaging of an outdoor scene using sunlight and the IDH system. As another way, IDH has also been implemented with Mach-Zehnder-type radial shearing self-interference interferometer by many researchers (Pedrini et al., 2012; Naik et al., 2014). Furthermore, a unique IDH technique exploiting the nature of coherence has been proposed by Takeda *et al.*, which is termed Coherence holography (Takeda et al., 2005; Naik et al., 2009).

A self-interference IDH system using an image sensor described above adopts one of two-arm interferometers and tolerance against external vibration is a serious problem. It is said that an IDH system has been constructed on a wagon table to record phase-shifted incoherent holograms of an outdoor scene. However, motion-picture recording for the scene has not been successfully demonstrated until now. It seems that this is because it is difficult to stably record phase-shifted holograms. Therefore,

such IDH systems have been constructed on an anti-vibration table to obtain the reproductivity. On the other hand, a single-path self-interference IDH system is highly stable and enables us to construct an IDH system on a commonly used table. It is notable that such a phase-shifting IDH system using an image sensor was, in my knowledge, initially proposed in 1990s, based on CH (Mugnier and Sirat, 1992; Mugnier et al., 1993; Mugnier, 1995). In this section, we describe CH as an important single-path polarimetric interferometer and then IDH techniques with a single-path interferometer and an image sensor.

2.1 Conoscopic Holography

CH (Sirat and Psaltis, 1985) was proposed for recording 3D information of incoherent light as an incoherent hologram. The main feature of CH is that it enables us to construct a compact single-path incoherent holography system by exploiting the polarization of light. CH is also useful for IDH and we briefly explain the technique. **Figure 2** illustrates the schematic of CH. In the initially proposed system (Sirat and Psaltis, 1985), between an incoherent object-wave point and an image sensor, a polarizer, a birefringent material, and an analyzer are set to generate self-



interference light of the object wave as shown in **Figure 2**. A polarizer aligns the polarization direction of the object wave. A birefringent material such as a crystal introduces different wavefront modulations against the orthogonally polarized light waves. In **Figure 2**, a birefringent material has fast and slow axes for vertical and horizontal directions. Two wavefronts of vertically and horizontally polarized object waves are generated from an object wave. Different wavefront curvature radii are introduced to the orthogonal polarizations when using a birefringent lens or a thick birefringent plate. An analyzer aligns the polarization directions of the two waves, and the two waves interfere with each other when the optical-path-length difference is carefully adjusted. A recording material such as a photographic plate and a film records an interference fringe image. Here, a 3D object illuminated by spatially incoherent light is regarded as the summation of spatially incoherent object-wave points in 3D space. Therefore, incoherent superpositions of GZP patterns of multiple object-wave points are formed on the recording material, and the formed image is recorded as an incoherent hologram of the 3D object. A 3D image of the object is optically reconstructed using the recorded incoherent hologram. Undesired-order diffraction images such as zeroth-order diffraction light and the conjugate image are suppressed with optical filtering in CH. A clear interference fringe pattern is formed owing to the proposed single-path polarimetric interferometer. Then, CH has adopted PSI with the designed PSI method to remove undesired-order diffraction waves. **Figure 2B** illustrates its schematic. A liquid crystal phase modulator and a designed amplitude mask attached with a rotational stage are set to conduct the designed PSI. The detailed explanations can be seen in refs. (Mugnier and Sirat, 1992; Mugnier et al., 1993; Mugnier, 1995). It is notable that phase-shifting DH was proposed and implemented for CH and spatially incoherent light before the proposal of famous phase-shifting DH using a laser (Yamaguchi and Zhang, 1997).

2.2 Fresnel Incoherent Correlation Holography

FINCH (Rosen and Brooker, 2007; Rosen et al., 2019) is an IDH technique exploiting a phase-only SLM and digital signal

processing based on DH with PSI. Instead of a solid birefringent material, FINCH adopts a diffractive optical element as shown in **Figure 3**. A liquid crystal on silicon SLM (LCoS-SLM) is set to generate two object waves with different wavefront curvature radii. Phase-shifted Fresnel phase lens patterns are displayed on the LCoS-SLM, and phase-shifted incoherent holograms are sequentially recorded by changing the phases of the phase lenses. A compact single-path phase-shifting IDH system has been realized by exploiting the LCoS-SLM as a two-wavefront generator and a phase shifter. Space-division (Rosen and Brooker, 2007) and polarization (Brooker et al., 2011) multiplexing techniques were proposed to generate two waves. PSF improvement in incoherent imaging was clarified after the experimental demonstrations (Rosen et al., 2011). FINCH has clarified that IDH is effective for not only incoherent holographic 3D imaging but also improving the resolution in general incoherent imaging techniques.

2.3 Computational Coherent Superposition Incoherent Digital Holography

DH techniques that are invented in laser holography contribute to the development of IDH. OSH and FINCH have demonstrated incoherent 3D imaging without undesired-order diffraction images by applying digital signal processing based on interferometry. Progress on laser DH techniques is continuing, and PSI selectively extracting wavelength information was invented (Tahara et al., 2015a; Tahara et al., 2015b; Tahara et al., 2017b; Tahara et al., 2018a). Not only 3D information but also wavelengths and polarization directions are simultaneously and selectively extracted with PSI by introducing different phase shifts for different physical information (Tahara et al., 2018a). Therefore, multidimensional information (3D space, phase, wavelengths, and polarization) are multiplexed on the image sensor plane with phase shifts and individually reconstructed by applying the PSI technique. This PSI is termed the computational coherent superposition (CCS) scheme and CCS has been applied to IDH (Tahara et al., 2019; Tahara et al., 2020b; Hara et al., 2020; Tahara et al., 2021a; Tahara et al., 2021b). **Figure 4** shows the schematic of CCS applied to IDH. CCS-IDH is implemented with arbitrary IDH systems that adopt PSI. **Figures 4A,B** are the combinations of CCS with FINCH and CH, respectively. The main difference of CCS from CH and FINCH is the recording of wavelength-multiplexed phase-shifted incoherent holograms. Wavelength information is simultaneously recorded without changing optical filters and obtained with digital signal processing based on CCS. The combination of CCS and FINCH is implemented by introducing an LCoS-SLM whose phase modulation range is sufficiently wide to apply a CCS algorithm (Hara et al., 2020). This is because different phase shifts for different wavelength bands should be introduced in CCS. The LCoS-SLM displays phase-shifted Fresnel phase lens patterns that are required for CCS-FINCH. The high spatial resolution of an LCoS-SLM enables us to generate fine interference fringes and to conduct high-resolution incoherent holographic 3D imaging. However, a

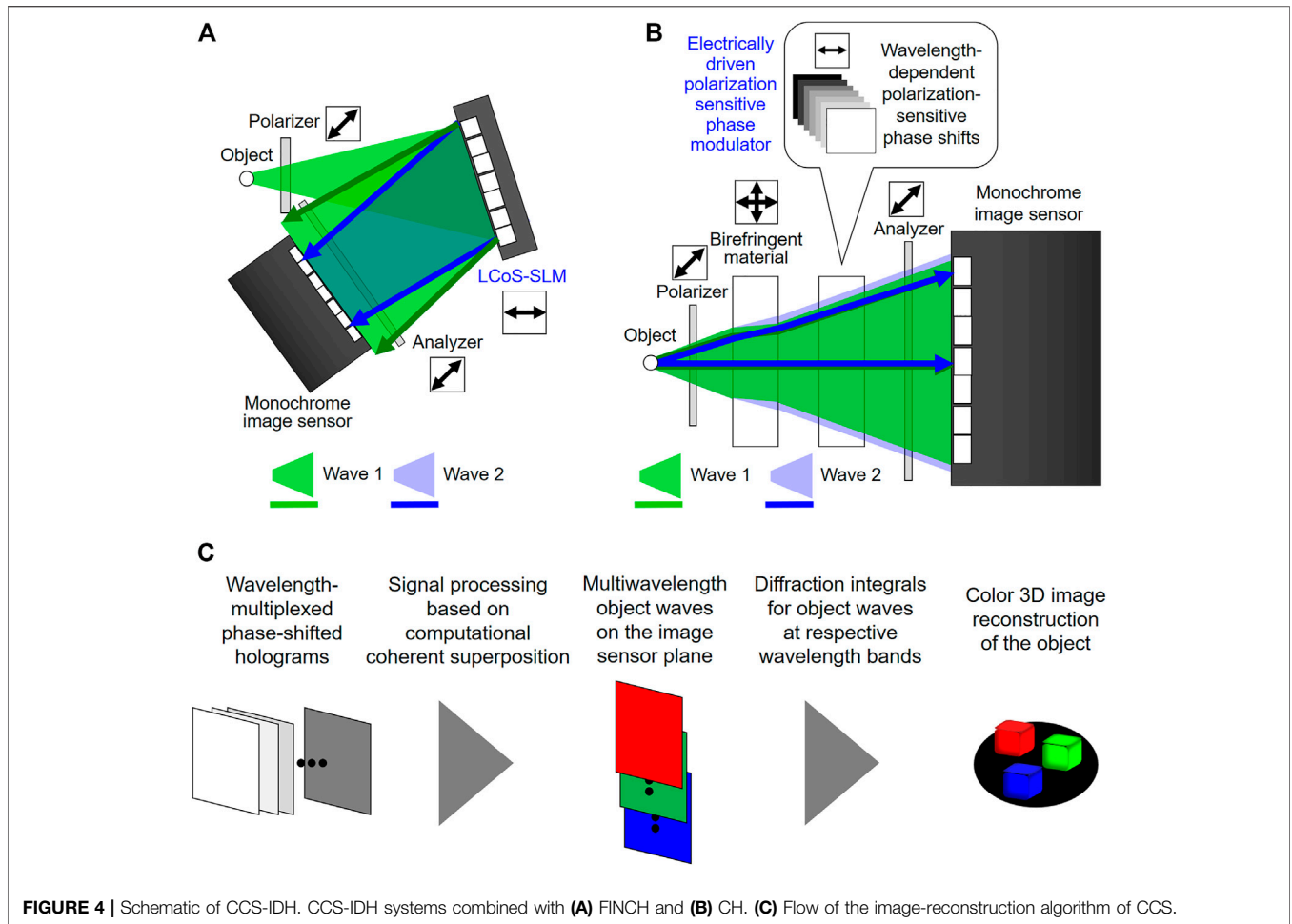


FIGURE 4 | Schematic of CCS-IDH. CCS-IDH systems combined with (A) FINCH and (B) CH. (C) Flow of the image-reconstruction algorithm of CCS.

diffractive optical element has strong selectivity and dependence in wavelength. A Fresnel phase lens works as a lens correctly only for the designed wavelength. Diffraction efficiency is decreased, and undesired-order diffraction waves are generated, as the wavelength of the incident light is different from the designed wavelength. Such a problem causes multiple object-image generations and image-quality degradations. To solve this problem, CCS is combined with CH as another optical implementation as shown in **Figure 4B** (Tahara et al., 2019; Tahara et al., 2020b; Tahara et al., 2021a; Tahara et al., 2021b). The combination of CCS with CH is implemented by inserting an electrically driven polarization-sensitive phase modulator such as a liquid crystal phase retarder or a nonlinear optical element. A liquid crystal generally has wavelength dependence for phase shifts and therefore applicable to phase encoding required for CCS. An SLM is not always required when using the IDH system shown in **Figure 4B**. **Figure 4C** illustrates the flow of the image-reconstruction algorithm of CCS-IDH. From the recorded wavelength-multiplexed phase-shifted incoherent holograms, multiwavelength object waves are selectively extracted using a CCS algorithm. As mathematical expressions, where $A_{ok}(x, y)$ and $\phi_k(x, y)$ are respectively the amplitude and phase distributions at wavelength λ_k , $k = 1, \dots, N$ is the number of the wavelength bands, α_{kl} is the l th phase shift at a wavelength λ_k ,

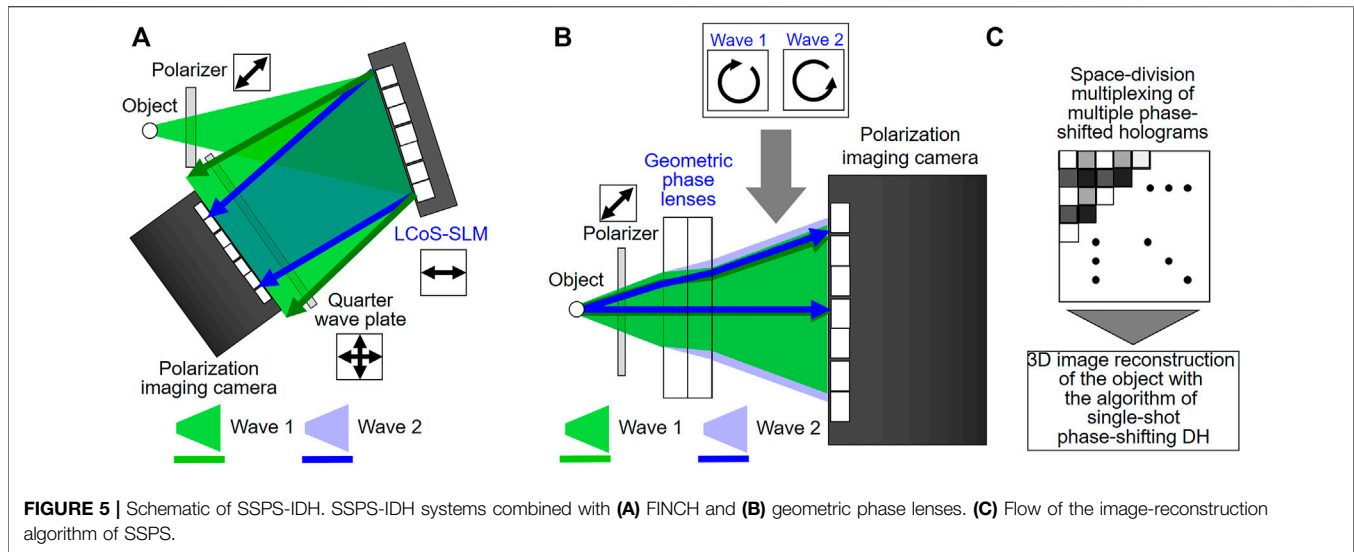
C_k is a coefficient, j is the imaginary unit, and $I_{0th}(x, y)$ is the summation of zeroth-order diffraction waves, the relationship between $I(x, y; \alpha_{1l}, \dots, \alpha_{kl}, \dots, \alpha_{Nl})$ and complex amplitude distributions at wavelengths $U_k(x, y) = C_k A_{ok}(x, y) [\cos \phi_k(x, y) + j \sin \phi_k(x, y)]$ is expressed as

$$I = PU, \tag{1}$$

where

$$I = \begin{pmatrix} I_1(x, y) \\ I_2(x, y) \\ I_3(x, y) \\ \vdots \\ I_{2N}(x, y) \\ I_{2N+1}(x, y) \end{pmatrix}, \tag{2}$$

$$P = \begin{pmatrix} 1 & 1 & 0 & \dots & 1 & 0 \\ 1 & \cos \alpha_{11} & \sin \alpha_{11} & \dots & \cos \alpha_{N1} & \sin \alpha_{N1} \\ 1 & \cos \alpha_{12} & \sin \alpha_{12} & \dots & \cos \alpha_{N2} & \sin \alpha_{N2} \\ \vdots & \vdots & \vdots & \ddots & \vdots & \vdots \\ 1 & \cos \alpha_{1(2N-1)} & \sin \alpha_{1(2N-1)} & \dots & \cos \alpha_{N(2N-1)} & \sin \alpha_{N(2N-1)} \\ 1 & \cos \alpha_{1(2N)} & \sin \alpha_{1(2N)} & \dots & \cos \alpha_{N(2N)} & \sin \alpha_{N(2N)} \end{pmatrix}, \tag{3}$$



$$U = \begin{pmatrix} I_{0th}(x, y) \\ C_1 A_{o1}(x, y) \cos \phi_{o1}(x, y) \\ C_1 A_{o1}(x, y) \sin \phi_{o1}(x, y) \\ \vdots \\ C_N A_{oN}(x, y) \cos \phi_{oN}(x, y) \\ C_N A_{oN}(x, y) \sin \phi_{oN}(x, y) \end{pmatrix}, \quad (4)$$

Then, complex amplitude distributions at multiple wavelengths are derived by solving

$$U = P^{-1}I, \quad (5)$$

Equation 5 means that object waves at multiple wavelengths are selectively extracted from multiplexed holograms using CCS. Diffraction integrals are calculated for the retrieved multiwavelength object waves, and a multiwavelength 3D image of the object is reconstructed.

It is noted that phase shifts are introduced to respective wavelengths simultaneously. Arbitrary phase shifts can be set to $\alpha_{1b} \dots, \alpha_{Nl}$ in **Eq. 3**. When P is a regular matrix, N -wavelength object waves are generally derived from $2N + 1$ wavelength-multiplexed phase-shifted holograms. A small condition number of P should be selected for a CCS algorithm, and phase shifts to set a small condition number should be designed for high-quality imaging. The image quality becomes higher as the condition number becomes smaller. The design of the smallest P using the prepared phase shifter and the measured wavelengths is effective. This is due to the numerical stability of a CCS algorithm and finite signal-to-noise ratio and finite bit depth of the recorded digital images.

2.4 Single-Shot Phase-Shifting Incoherent Digital Holography

Single-shot phase-shifting (SSPS) DH (Zhu and Ueda, 2003; Millerd et al., 2004; Awatsuji et al., 2004) is a technique used in laser holography and has been applied to IDH (Tahara et al.,

2017a; Nobukawa et al., 2018; Choi et al., 2019; Liang et al., 2020; Tahara et al., 2020a). Several optical implementations have been presented in IDH to date. **Figure 5** shows examples of optical implementations in SSPS-IDH. SSPS-IDH can be implemented with the combinations of optical systems in SSPS with FINCH (Tahara et al., 2017a; Tahara and Sato, 2019), geometric phase lens (es) (Choi et al., 2019; Liang et al., 2020; Tahara et al., 2020a), and a grating (Nobukawa et al., 2018). SSPS is implemented using the polarization of interference light and a polarization-imaging camera (Millerd et al., 2004). FINCH also utilizes polarization light and can be easily combined with SSPS as shown in **Figure 5A** (Tahara et al., 2017a; Tahara and Sato, 2019). On the other hand, the use of a geometric phase lens for IDH was proposed and then several IDH systems have been presented (Choi et al., 2019; Liang et al., 2020; Choi et al., 2018). A geometric phase lens generates two circularly polarized light waves whose polarization is orthogonal. This feature is suitable for implementing self-interference DH with SSPS and therefore applicable to SSPS-IDH. After that, a thin SSPS-IDH system without a refractive lens was proposed as shown in **Figure 5B** (Tahara et al., 2020a; Tahara and Oi, 2021). In SSPS, multiple phase-shifted holograms are simultaneously recorded by space-division multiplexing as shown in **Figure 5C** (Zhu and Ueda, 2003; Awatsuji et al., 2004; Millerd et al., 2004). A de-mosaicking procedure is conducted in a computer, and then an image-reconstruction algorithm of PSDH is applied with multiple de-mosaicked holograms to reconstruct a holographic 3D image of the object. Note that single-shot incoherent holographic 3D imaging is conducted with a compact single-path IDH system (Tahara and Oi, 2021).

3 APPLICATIONS OF INCOHERENT DIGITAL HOLOGRAPHY

IDH has potential to considerably extend the applicability of DH. Laser light is no longer mandatory when using IDH. Any light

source including self-luminous light and natural light can be recorded as a hologram. Various techniques such as 3D microscopy for self-luminous light (Schilling et al., 1997; Rosen and Brooker, 2008; Jang et al., 2015; Yanagawa et al., 2015; Quan et al., 2017; Liebel et al., 2020a; Liebel et al., 2020b; Kumar et al., 2020; Marar and Kner, 2020; Potcoava et al., 2021), 3D imaging with a single image sensor (Kim, 2013; Clark and Kim, 2015; Jang et al., 2015; Vijayakumar et al., 2016; Vijayakumar and Rosen, 2017; Nobukawa et al., 2018; Choi et al., 2019; Nobukawa et al., 2019; Wu et al., 2020; Tahara et al., 2021d; Wu et al., 2021; Yoneda et al., 2021; Tahara et al., 2022), 3D thermal measurement (Imbe, 2019), and spectroscopic 3D imaging (Yoshimori, 2001; Teeranutrannont and Yoshimori, 2013; Naik et al., 2014; Kalenkov et al., 2019) have been proposed to date. Research on applications of IDH is ongoing and a challenging theme. In this section, applications of IDH to multidimensional microscopy and the holoSensor are presented.

3.1 Incoherent Digital Holographic Microscopy: Microscopy Application of Incoherent Digital Holography

Incoherent digital holographic microscopy (IDHM) is considered a prospective application of IDH. In the field of microscopy, it is important to record both 3D information and wavelength information simultaneously with weak illumination-light intensity and a compact optical setup. In the fluorescence microscopy application, wavelength information is used as the label for molecule compositions. Measurements with weak illumination-light intensity are required to suppress phototoxicity in cells and to conduct high-speed sensing of molecules. Full-color 3D imaging and restoration as quantitative and digital information are also highly required for Raman scattering microscopy and the widely used optical microscopy with a halogen lamp. Hyperspectral incoherent holography with a two-arm interferometer has been proposed as a conventional spectroscopic and incoherent holographic 3D imaging technique (Yoshimori, 2001; Teeranutrannont and Yoshimori, 2013; Naik et al., 2014; Kalenkov et al., 2019). However, tolerance against vibrations is low owing to the use of a two-arm interferometer. However, two arms were required to adopt a temporal heterodyne technique in IDH with the Fourier spectroscopy. To solve this problem is one of the challenging research topics in multiwavelength IDH. In this section we present several ways to solve this problem.

3.1.1 CCS Incoherent Digital Holographic Microscopy

We can realize spectroscopic IDHM with high tolerance against external vibrations, using CCS-IDH. We have constructed a CCS-IDHM system that is shown in **Figure 6** to apply a novel type of spectroscopic IDHM. CCS-IDHM is composed of a CCS-IDH system and an incoherent optical microscope (Tahara et al., 2020b; Tahara et al., 2021a; Tahara et al., 2021b). An optical microscope with incoherent light such as self-luminous light including fluorescence light, Raman scattering light, thermal light generated from a halogen lamp, and light generated from a light-emitting diode (LED) can be combined with a CCS-IDH system. The magnified 3D image of a specimen is irradiated from

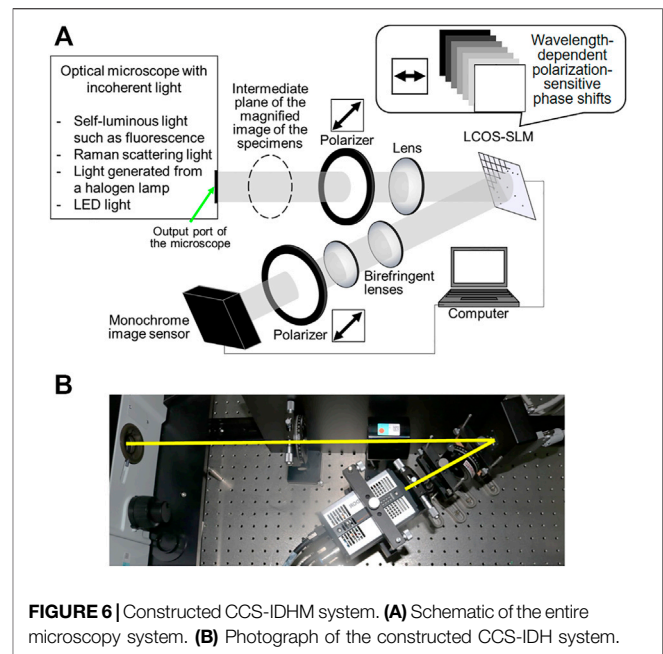
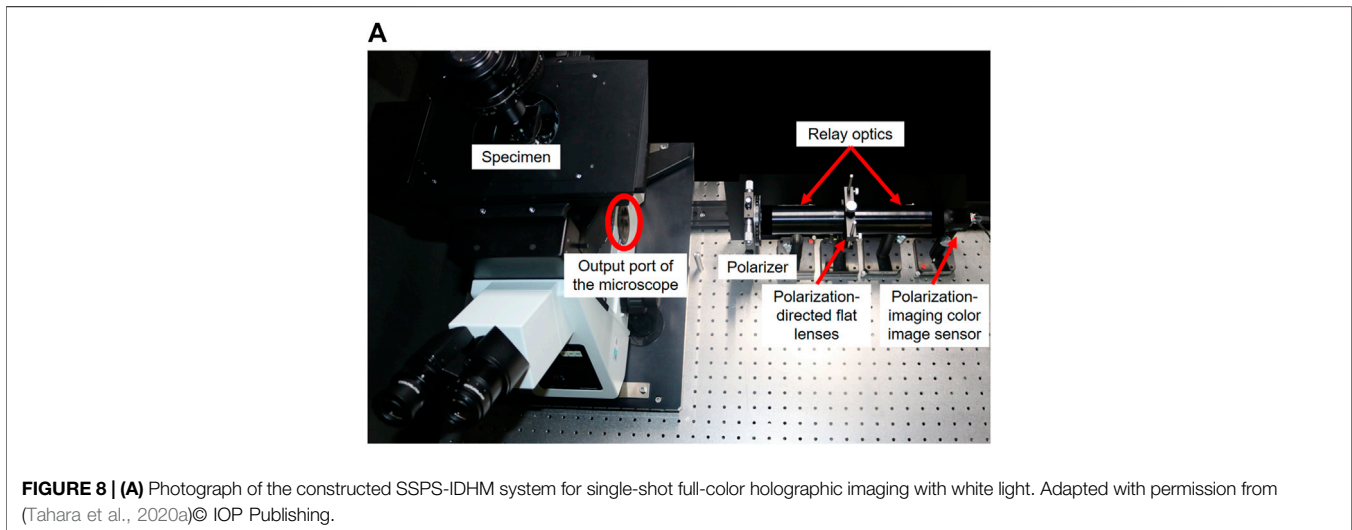
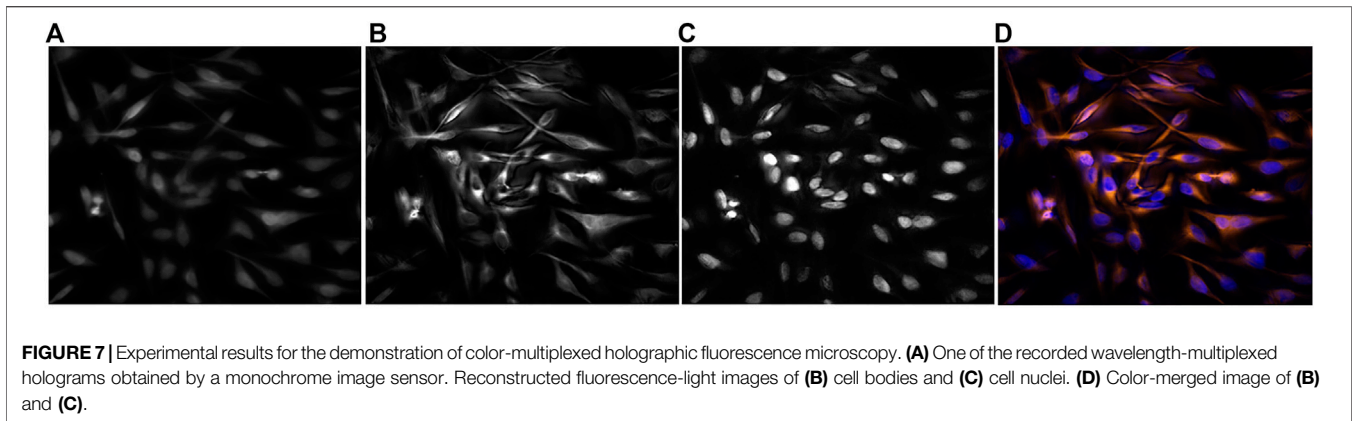


FIGURE 6 | Constructed CCS-IDH system. **(A)** Schematic of the entire microscopy system. **(B)** Photograph of the constructed CCS-IDH system.

the output port of the microscope, and the magnified 3D image that is focused on the intermediate plane is treated as the 3D specimen in the CCS-IDH system. **Figure 6** also shows the single-path wavelength-multiplexed IDH system constructed as described in **section 2.3**, which provides high tolerance against vibrations in spectroscopic holographic interferometry. A full-color holographic 3D microscope with a halogen lamp and a multiband-pass filter was constructed to first demonstrate CCS-IDHM (Tahara et al., 2020b). Experiments on HE-stained mouse kidney cells were successfully conducted. Then, PSF improvement in full-color incoherent imaging was achieved (Rosen et al., 2021). The CCS-IDH system was also combined with a fluorescence microscope, and color-multiplexed holographic fluorescence microscopy was presented (Tahara et al., 2021a; Tahara et al., 2021b). In the experimental demonstration, fluorescence-stained HeLa cells were prepared. Cell nuclei and cell bodies were stained by different fluorescence markers. As a result, different molecule compositions were labelled by different fluorescence light wavelengths. Detailed conditions for cell staining and the constructed optical setup were described in (Tahara et al., 2021a). **Figure 7** shows the experimental results, which indicate that a monochrome image sensor records wavelength-multiplexed fluorescence holograms, and wavelengths are successfully separated by the CCS. Different molecule compositions are separately obtained by wavelength separations, and focused color fluorescence images of the cells are reconstructed. It is expected that CCS-IDHM is applied to spontaneous Raman imaging and works as multicolor holographic Raman scattering microscopy with a single-path wavelength-multiplexed interferometer.

3.1.2 Full-Color SSPS-IDHM With White Light

Utilization of SSPS-IDH is also effective as another way to realize multiwavelength IDHM with high tolerance against external



vibrations. Currently, one can construct an SSPS-IDH system (Tahara et al., 2017a; Nobukawa et al., 2018; Choi et al., 2019; Liang et al., 2020; Tahara et al., 2020a; Tahara and Sato, 2019). Optical components and a polarization-imaging camera shown in **Figures 5A,B** are commercially available and can be obtained at a low cost. In comparison to CCS-IDHM, higher-temporal resolution is obtained using SSPS-IDHM with a color polarization-imaging camera. Full-color holographic 3D imaging with SSPS-IDHM and a halogen lamp was experimentally demonstrated. **Figure 8A** shows a photograph of one of the constructed SSPS-IDHM systems. The constructed system is composed of an optical microscope with a halogen lamp and an SSPS-IDH system. The SSPS-IDH system treats the magnified 3D image that is focused on the intermediate plane as the 3D specimen. In the constructed SSPS-IDH system, the relay optics is set to collect the light wave of the magnified specimen and to conduct Fourier transform (FT) and inverse FT optically. Polarization-directed flat lenses that are ones of geometric phase lenses are set on the FT plane of relay optics for shift-invariant PSF engineering. A red, green, and blue (RGB) color-filter array of a polarization-imaging color camera selects a wavelength band from the continuous spectral bandwidth of white light generated from a halogen lamp. RGB channels of the

color-filter array select the corresponding RGB wavelength bandwidths. The selected bandwidths are within 100 nm. With the color-filter array, not only RGB color information is obtained but also temporal coherency is improved. Detailed experimental conditions are described in (Tahara et al., 2020a). **Figure 9** shows the experimental results, which indicate that both color information and 3D information are reconstructed from the recorded single incoherent hologram. Defocused images on the image sensor plane can be seen at red and green channels, although a focused image was obtained at the blue channel as shown in **Figures 9A–C**. This is attributable to the chromatic aberration of optical elements in the constructed SSPS-IDH system. However, focused images at RGB channels are obtained by the digital refocusing of DH as shown in **Figures 9D–G**. The results indicate that aberration can be compensated with digital signal processing based on holography. Thus, single-shot incoherent color 3D imaging of the specimen is successfully performed. An application to color holographic fluorescence microscopy was also attempted.

3.1.3 The Combination of CCS and SSPS for IDHM

Single-shot wavelength-multiplexed IDH is realized by combining CCS-IDH and SSPS-IDH (Tahara et al., 2020c).

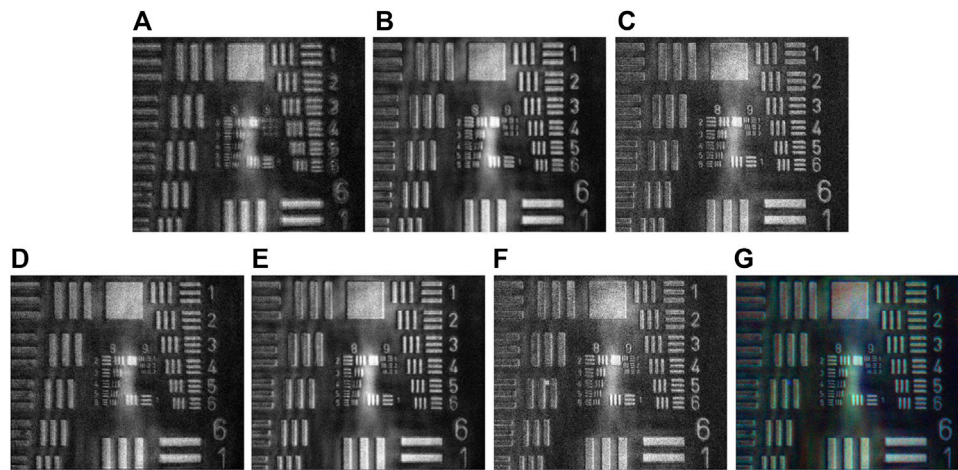


FIGURE 9 | Experimental results of full-color imaging of USAF1951 test target. Images reconstructed on the image sensor plane at (A) red, (B) green, and (C) blue channels. Images numerically focused on the magnified image plane at (D) red, (E) green, and (F) blue channels. (G) Color-synthesized image from (D–F). Adapted with permission from (Tahara et al., 2020)© The Optical Society.

Here, we call the combined technique single-shot CCS (SS-CCS) IDH. **Figure 10** shows the schematic of the SS-CCS IDH. Light generated from objects/specimens is converted two light waves by an IDH system using polarization. A monochrome image sensor with a wavelength-dependent polarization-sensitive phase-modulation (WPP) array and a polarizer records two light waves as a wavelength-multiplexed self-interference hologram. In the recorded hologram, the information of multiple wavelength-multiplexed holograms required for CCS is contained, based on space-division multiplexing of holograms. Instead of a micropolarizer array, a WPP array is inserted to apply both CCS and SSPs. De-mosaicking procedure used for pixelated/parallel PSI can also be applied to the recorded single image and then complex amplitude distributions at multiple wavelengths are retrieved using a CCS algorithm. A multiwavelength 3D image is reconstructed by numerical focusing such as diffraction integrals.

A WPP array was developed to combine the two IDH techniques. **Figure 11** shows the schematic of the WPP array and a photograph of the image sensor with the WPP array. Each WPP cell is composed of a photonic crystal, and a photonic-crystal array is fabricated by the self-cloning technique (Sato et al., 2007). The phase shifts of cells A, C, D, and E at the wavelength of 532 nm are 240, 107, 213, and 320°. Wavelength dependency of the phase shift of the photonic crystal fabricated is used for a CCS algorithm. More detail of the developed image sensor is described in ref. (Tahara et al., 2020c). We have constructed an SS-CCS IDHM system to experimentally show its validity, which is the combination of a fluorescence microscope, a CCS-IDH system, and the image sensor. Detailed experimental conditions are described in (Tahara et al., 2020c). Experimental results shown in **Figure 12** indicate that fluorescence object waves at different wavelength bands are selectively extracted, and 3D information at respective wavelength bands is reconstructed successfully. Different types of fluorescence particles are identified using wavelength separations with CCS. Experimental results show

that SS-CCS IDHM performs color 3D imaging of fluorescence light from the single wavelength-multiplexed hologram. Improvements of image quality and frame rate are ongoing, and color 3D motion-picture recording of incoherent holograms with more than 70 fps and 4 megapixels has been performed to date (Tahara et al., 2021).

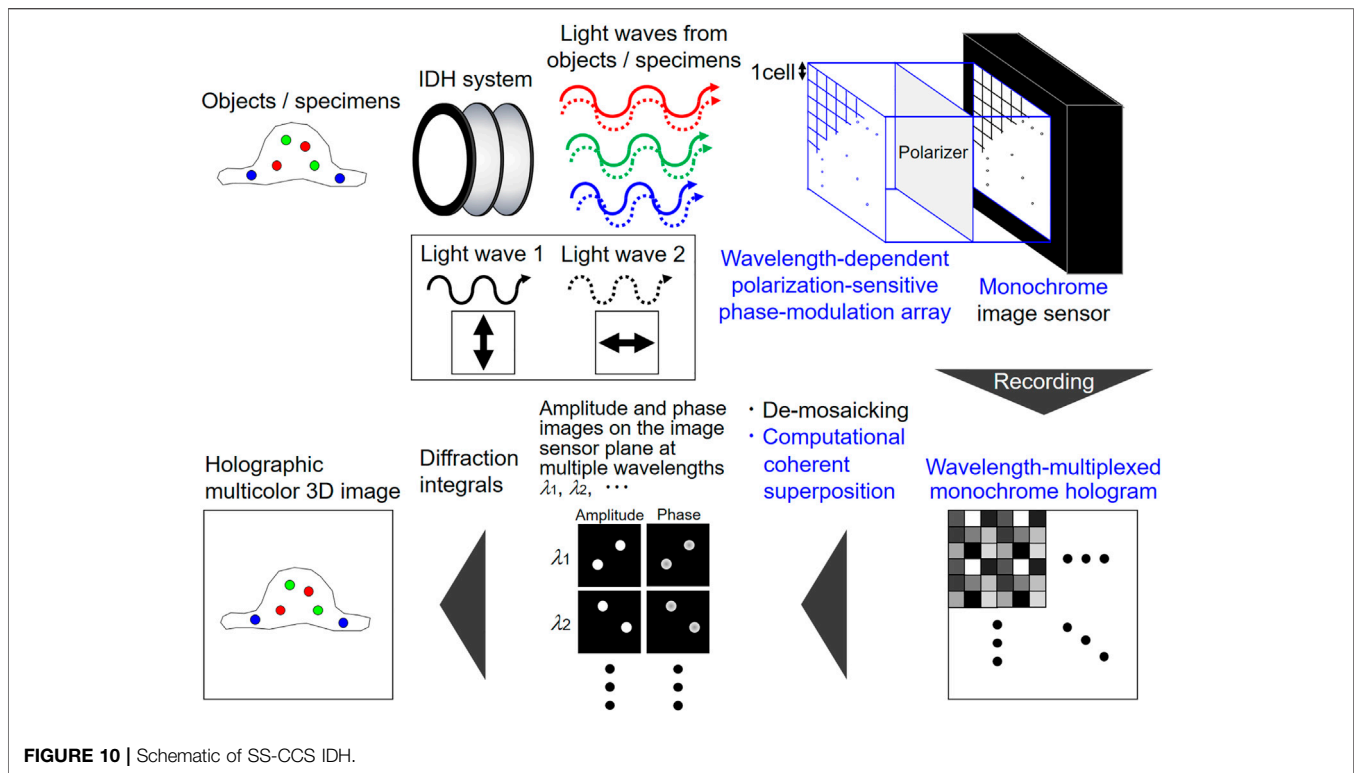
3.2 Compact Hologram Recorder—Holo-sensor—

As described in the **section 2**, an IDH system can be constructed with a small-size optical setup. A compact and portable hologram recorder is strongly desired in many fields of scientific research and industry. We introduce our compact hologram recorders, which is termed holo-sensor.

3.2.1 Multiplexed Holo-sensor Based on CCS-IDH

CCS-IDH is implemented with a compact optical system by adopting CH without an amplitude mask. In previous sections, we have shown how a compact system can be constructed in comparison with a two-arm laser interferometer. However, a more compact optical system can be constructed. **Figure 13A** shows the schematic of the basic concept of the ultimately compact hologram recorder based on CCS-IDH (Tahara, 2021; Tahara et al., 2021; Tahara et al., 2021c). Such a hologram recorder is composed of the integrations of the optical elements shown in **Figure 4B**. As a first step, we have succeeded in designing and constructing the holo-sensor as shown in **Figures 13B,C**. Experimental results with the prototypes of the CCS-holo-sensor can be seen in (Tahara et al., 2021; Tahara et al., 2021c).

Color imaging and 3D imaging have been performed using the developed CCS-holo-sensors (Tahara et al., 2021; Tahara et al., 2021c). However, several research topics are raised. Measurement speed is closely related to the speed of phase shifts and the frame rate. A compact and transparent polarimetric phase modulator is commercially available. A liquid crystal is used for such a phase



modulator, and its working speed is much lower than the video rate. Although the working speed is much improved by using a high-speed LCoS-SLM, the size of the CCS-holosensor is increased. The size is also increased when using a Faraday rotator (Ueda and Takuma, 1984). A high-speed, compact, and transparent polarimetric phase modulator is strongly desired for the CCS-holosensor. Otherwise, an architectural design for constructing a compact optical system with an LCoS-SLM is required. As another research theme, careful design of birefringent materials is important. The resolution of IDH is closely related to the pitch of interference fringes. A curvature-radius difference between the two object waves should be large to generate a fine interference fringe image. A transparent material with a large birefringence is effective for the generation of a fine interference fringe image. However, the optical-path-length difference increases as the curvature-radius difference increases. The coherence length is small in IDH and interference fringes easily disappear. Therefore, the optical-path-length difference is adjusted by inserting a birefringent phase plate. After that, an image sensor to record a fine interference fringe image should be selected, considering the sampling theorem.

The initially developed wavelength-multiplexed holosensor is palm-sized. Phase-shift error owing to vibrations was a serious problem in two-arm laser holography with CCS. Accurate phase shifts are mandatory for CCS, and object-wave extraction at the desired wavelength easily fails if a phase-shift error occurs. A single-path IDH system achieved high tolerance against vibrations and reduction of phase-shift error during recording of holograms. Integrations of optical elements and construction of an extremely compact optical system will further help to achieve accurate multidimensional measurement with CCS. A

chip-sized hologram recorder will be realized in the near future by integrating the optical elements.

3.2.2 Single-Shot Holo-sensor Based on IDH With SSPS and SS-CCS

A single-shot multidimensional compact hologram recorder can be fabricated using IDH with SSPS and SS-CCS. **Figure 14** illustrates the schematics. These systems can be constructed by integrating optical elements in the optical systems of SSPS and SS-CCS IDH. **Figure 14A** shows the integrated system shown in **Figure 5**. **Figure 14B** is the combination of **Figure 13A** and the image sensor with a WPP array. The finest pitch of interference fringes is determined by the design of birefringent materials and the pixel pitch of each phase-shifted holograms. A palm-sized single-shot holosensor can be constructed using commercially available optical elements and a polarization-imaging camera. As an experimental demonstration, we have developed a prototype of a single-shot holosensor based on SSPS as shown in **Figure 15A** (Tahara and Oi, 2021). With this single-shot holosensor, an object wave generated with an LED is recorded with a single-shot exposure of an image sensor as shown in **Figure 15B**. A focused object image is successfully reconstructed from a pixelated incoherent image as shown in **Figure 15C**. Detailed experimental conditions are described in (Tahara and Oi, 2021).

4 DISCUSSION AND CONCLUSION

Various IDH techniques have been proposed and continuously researched to date. We discuss the comparative merits of the introduced multidimensional IDH techniques. **Table 1** shows the

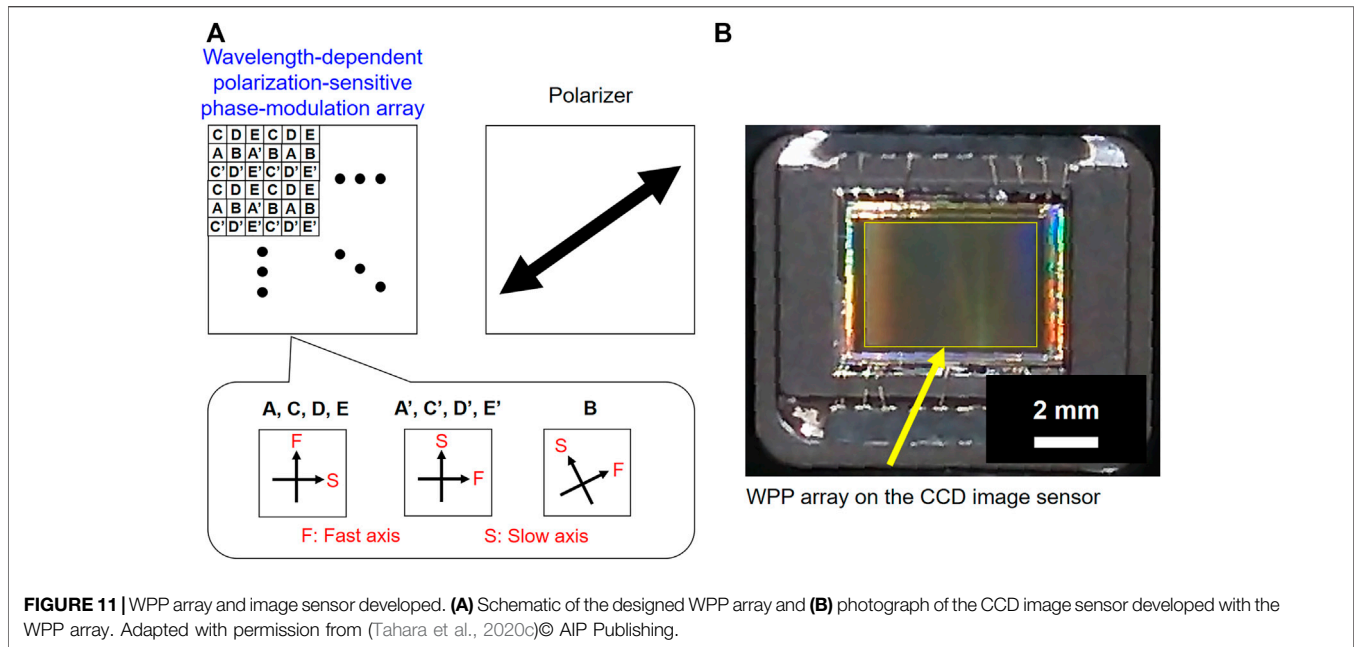
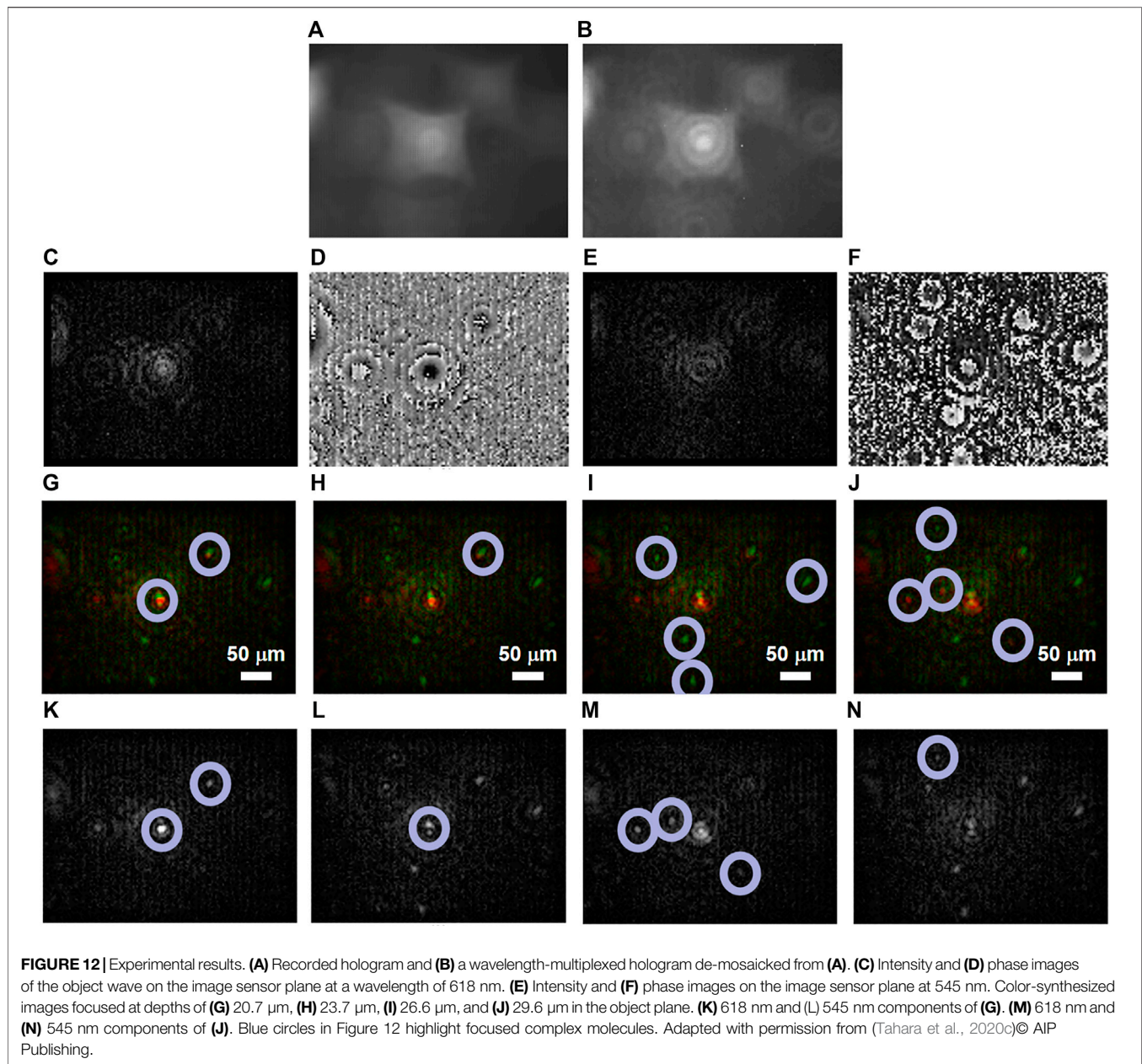


FIGURE 11 | WPP array and image sensor developed. **(A)** Schematic of the designed WPP array and **(B)** photograph of the CCD image sensor developed with the WPP array. Adapted with permission from (Tahara et al., 2020c)© AIP Publishing.

characteristics of various IDH techniques on tolerance against vibrations and information capacities for spatial, temporal, and wavelength imaging. Firstly, we discuss tolerance against vibrations and spatial and temporal information capacities. Spatial and temporal specifications of OSH depend on the range and speed of scan of illumination light and pitch of a GZP pattern. Tolerance against external vibrations is improved using a temporal heterodyne technique. CH is a spatially incoherent polarimetric phase-shifting DH technique. However, the use of a birefringent lens is not adopted. As a result, the resolution is limited although 3D imaging has been performed successfully. IDH has been implemented with various two-arm interferometers and many research achievements have been reported. However, tolerance against external vibrations is a problem. Coherence holography adopts Sagnac interferometer and is highly tolerant to external vibrations. Single-shot holographic imaging of spatially incoherent light has been demonstrated experimentally using an off-axis interferometer (Takeda et al., 2005; Naik et al., 2009) and therefore high temporal information capacity is obtained. On the other hand, spatial information capacity is limited owing to the use of an off-axis geometry. FINCH has clarified that, light sources with limited temporal coherency such as a lamp and an LED are recorded with a bandpass filter as holograms and in-plane PSF is improved at the cost of depth resolution. FINCH has been combined with PSI and off-axis holography. Therefore, spatial and temporal information capacities are flexibly designed. COACH improves depth resolution in comparison to self-interference DH with radial shearing. However, the acquisition of a PSF library on the measured 3D area is required. In IDH with a spatially incoherent light source containing single wavelength band, SSPS-IDH has contributed to the improvement of the product of spatial and temporal information capacities. Single-shot

imaging can be conducted with an in-line configuration by using SSPS. In comparison to the off-axis geometry, space-bandwidth product (SBWP) is improved, and the visibility of interference fringes is improved by using an in-line configuration. As a result, field of view (FOV) extension owing to the increase of the SBWP and image-quality improvement owing to the enhancement of visibility are achieved in principle.

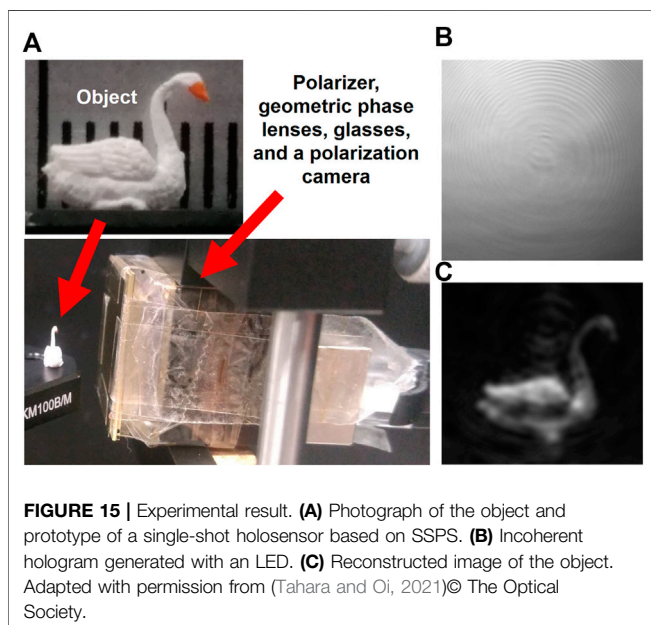
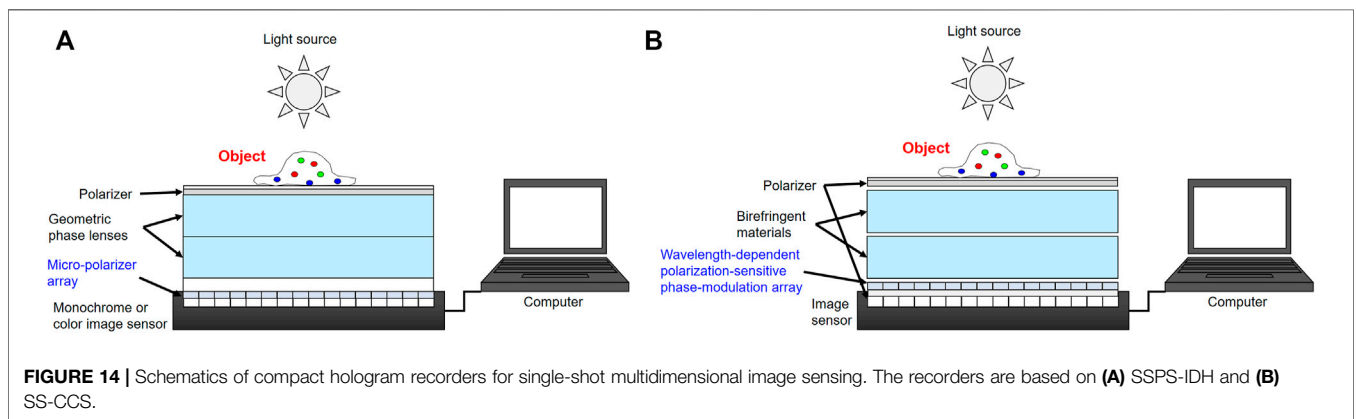
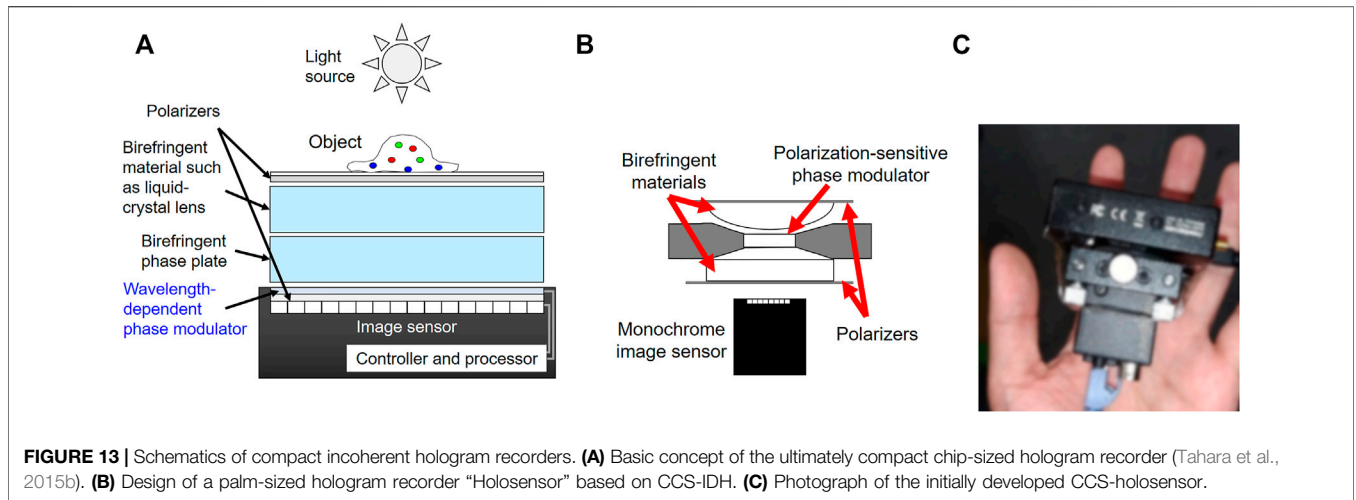
IDH for speckleless color holographic 3D imaging is a highly interested research theme. Using such an IDH technique, spatially and temporally incoherent light is recorded as incoherent hologram (s). Wavelength information is recorded using various wavelength-sensing techniques presented in DH (Tankam et al., 2010; Tahara et al., 2018b) and IDH adopts the techniques as shown in **Table 1**. Simultaneous RGB color sensing can be conducted using the principle of the Fourier spectroscopy. In OSH, when using a temporal heterodyne technique, different temporal frequencies of respective color GZP patterns are introduced and RGB information of the object is separated in the temporal frequency domain. The Fourier spectroscopy is also adopted to IDH with a two-arm interferometer. However, more than 250 exposures are required to conduct RGB color 3D imaging, and to reduce the number of exposures is a research problem when the number of the wavelength bands is small. FINCH adopts a diffractive phase lens and such a lens correctly works for the designed wavelength. Therefore, FINCH is not suitable for simultaneous multiwavelength measurement, and multiple bandpass filters and diffractive phase lenses are changed to obtain wavelength information sequentially. The filters should be sequentially changed using a filter wheel and this procedure loses temporal information capacity. The use of a color camera is straightforward and effective for color holographic imaging. On the other hand, spatial information capacity is partly lost when using a color camera with a color-filter



array. COACH utilizes wavelength dependency of a diffractive phase lens to separate wavelength information. The difference of the PSFs between different wavelength bands is used for the wavelength separation. FOV in the depth direction was limited but many researches are conducted to solve the problem. The main features of CCS-IDH are the single-path spectroscopic holographic interferometer with a phase modulator and wavelength separation with a small number of wavelength-multiplexed holograms. RGB holographic imaging has been conducted with seven wavelength-multiplexed holograms without a mechanical movement. The number of exposures is much less than that required for IDH adopting the Fourier spectroscopy when conducting RGB holographic imaging. Single-shot CCS is implemented using a WPP array, and

temporal information capacity is enhanced at the partly cost of spatial information capacity owing to space-division multiplexing. In comparison to IDH using an RGB color camera, SS-CCS IDH can improve the SBWP available for recording an RGB object wave. This is because the number of multiplexing is reduced, and spatial density of respective phase-shifted holograms is increased.

However, there are problems to limit the specifications of CCS-IDH, SSPS-IDH, and SS-CCS IDH. The research topics of CCS-IDH are described in the **section 3.2.1**. CCS-IDH will proceed toward a highly stable hyperspectral holographic 3D imaging technique and a phase modulator to enhance the specification of the technique will be a key optical device. An advanced signal-processing algorithm in CCS is also important to



enhance wavelength-sensing ability for IDH. In SSPS-IDH, a geometric phase lens is particularly useful for constructing a compact IDH system. A commercially available geometric phase lens is usable for white light. However, an undesired-order diffraction wave generated from the lens is not completely avoidable to date. Figure 9 shows an example. The residual light seen in the centers of **Figures 9A–G** is owing to the wave generated from the lens. Developments of some algorithms to remove such light are important to apply the SSPS-IDH system for scientific research. In SS-CCS IDH, the development of an advanced WPP array is important. Until now, it is difficult to attach an image sensor and a WPP array with a large number of cells and high spatial density.

Many IDH techniques have been proposed and developed as listed in **Table 1**. Experimental demonstrations of IDH techniques have been performed and various applications have been indicated with experimental results. However, researches and enhancements on IDH should be conducted toward applications to both scientific research and industry. Firstly, light-use efficiency should be improved toward the applications to fluorescence, Raman scattering, or other weak-

TABLE 1 | Comparisons of various IDH. *N* means the number of the wavelength bands measured.

	Tolerance against external vibrations	Monochrome imaging		Method to obtain wavelength information	RGB color imaging		Challenge to spectroscopic measurement
		Spatial information	Temporal information		Spatial information	Temporal information	
Optical scanning holography Poon and Korpel. (1979), Poon (1985)	High	Dependent on scan	Dependent on scan	Temporal frequency-division multiplexing	Dependent on scan	Dependent on scan	Requirement of multiple lasers
Conoscopic holography Sirat and Psaltis (1985), Mugnier and Sirat (1992), Mugnier et al. (1993), Mugnier (1995)	High	Difficulty in high resolution	Several exposures	—	—	—	—
IDH with a two-arm interferometer							
Rotational shearing Yoshimori (2001), Teeranuntranont and Yoshimori (2013) and Mach-Zehnder-type Pedrini et al. (2012), Naik et al. (2014)	Low	Full bandwidth	Several exposures	Temporal frequency-division multiplexing	Full bandwidth	More than 250 exposures	Acceleration of the measurement
Michelson-type with a concave mirror Kim (2012), Kim (2013), Clark and Kim (2015)	Low	Full bandwidth	Several exposures	Color camera with a color-filter array	A quarter of full bandwidth	Several exposures	Requirement of hyperspectral camera
Off-axis Michelson-type with a concave mirror Hong and Kim (2013)	Low	A ninth of full bandwidth	Single-shot exposure	—	—	—	—
Coherence holography Takeda et al. (2005), Naik et al. (2009) that adopts Sagnac interferometer	High	A ninth of full bandwidth	Single-shot exposure	—	—	—	—
Fresnel incoherent correlation holography Rosen and Brooker (2007), Rosen et al. (2011), Rosen et al. (2019)	High	Full bandwidth and PSF improvement	Several exposures	Use of multiple bandpass filters	Full bandwidth	3 <i>N</i> –4 <i>N</i> exposures	Requirement of multiple filters
Fourier incoherent single channel holography Kelner and Rosen (2012) and single-shot off-axis FINCH Quan et al. (2017)	High	A ninth of full bandwidth	Single-shot exposure	—	—	—	—
Coded aperture correlation holography Vijayakumar et al. (2016), Vijayakumar and Rosen (2017)	High	Full bandwidth	Several exposures	PSF engineering and a diffractive phase lens	FOV limited in the depth direction	Several exposures	Requirement of additional/modified signal processing
CCS-IDH Tahara et al. (2019), Tahara et al. (2020b), Hara et al. (2020), Tahara et al. (2021a), Tahara et al. (2021b)	High	—	—	Wavelength-dependent phase shifts	Full bandwidth	2 <i>N</i> + 1 exposures	Speed and range of phase modulation
SSPS-IDH Tahara et al. (2017a), Nobukawa et al. (2018), Choi et al. (2019), Tahara et al. (2020a), Liang et al. (2020)	High	A fourth of full bandwidth	Single-shot exposure	Color camera with a color-filter array	A 16th of full bandwidth	Single-shot exposure	Requirement of hyperspectral polarization-imaging camera
SS-CCS IDH Tahara et al. (2020c), Tahara et al. (2021)	High	—	—	Monochrome camera with a WPP array	A seventh of full bandwidth	Single-shot exposure	Development of an advanced WPP array

light nonlinear microscopy, and night-vision sensor. A polarimetric interferometer and a two-arm interferometer are frequently adopted in IDH. However, only a quarter of the intensity of the object wave can be utilized for the generation of an incoherent hologram in generally proposed IDH. An advanced optical system is effective for the improvement of the light-use efficiency. Furthermore, in the application to 3D fluorescence microscopy, light intensity is severely limited, and the number of photons in hologram recording should be

considered when conducting holographic measurements. The importance of quantum optics on weak-light holographic sensing for the estimation of holographic measurement accuracy (Okamoto and Tahara, 2021) will be further increased, particularly in IDH. Image-quality improvement is also important research theme. In IDH, visibility of a recorded incoherent hologram decreases as the size of the object increases. An image sensor with high dynamic range is used to obtain a high-quality incoherent hologram. However, higher dynamic

range is required to record an incoherent hologram of larger size of the object. As another research problem, most of self-interference incoherent DH has the problem of the depth resolution. PSF of the IDH system is generally not the same as that of DH with a plane reference wave. This is because a spherical wave whose wavefront curvature depends on the depth position of the object point is used to generate interference fringes in IDH. COACH can obtain higher depth resolution than FINCH and other many self-interference IDH techniques. However, PSF library is required in advance. Depth-resolution improvement by a simple method will extend applicability of IDH. As a demonstration for the applicability of IDH to depth imaging, the generation of a depth map from the recorded incoherent hologram(s) is also highly desired research topic. Quantitative visualization of depth information as a depth map was not strongly required in the field of IDH. In contrast, such a depth map has been generated in laser DH by using quantitative phase information and phase unwrapping. The importance on the generation of a depth map will be increased to indicate applicability to other research fields such as 3D particle and flow measurements, 3D surface inspection, and machine vision. The problem on the depth resolution will be indicated when the generation of a depth map.

As an additional discussion, we analyze the composition of the CCS-holosensor. The CCS-holosensor shown in Figure 13 is the combinations of CH, single-path spectroscopy exploiting polarization (Ueda and Takuma, 1984), and a PSI technique. Instead of a Faraday rotator used in ref. (Ueda and Takuma, 1984), a liquid crystal phase retarder is utilized as a wavelength-dependent polarization-sensitive phase modulator. Using a liquid crystal, the CCS-holosensor can work with low voltage and without additional controller. Instead of the use of single-wavelength PSI in IDH, which has been successfully performed by CH and FINCH (Mugnier and Sirat, 1992; Mugnier et al., 1993; Mugnier, 1995; Rosen and Brooker, 2007), multidimensional-multiplexed PSI termed CCS is adopted to conduct simultaneous multiwavelength holographic image sensing without changing optical filters such as color filters. The proposed CCS-holosensor is based on many pioneers including Lohman's idea for the use of a birefringent dual-focus lens. Considering the applications, the CCS-holosensor will be effective particularly for holographic sensing of multicolor self-luminous light. This is because one of the merits in IDH is to be able to acquire digital holograms of self-luminous light such as fluorescence light, which was initially performed by Poon *et al.* with OSH. Furthermore, CCS can perform the recording of multicolor fluorescence light as wavelength-multiplexed fluorescence digital holograms with a monochrome image sensor and no change of wavelength filters. Therefore, the CCS-holosensor will be able to work as an ultimately compact holographic fluorescence microscopy system. As another aspect, the CCS-holosensor can work as a compact spectroscopic

hologram recorder with self-luminous light including sunlight and Moon light. Compact IDH systems have been proposed using various IDH techniques, which is described in this review and ref. (Rosen et al., 2021). It is now possible to realize portable holographic imaging systems for sensing outdoor 3D scenes with IDH techniques. Using CCS-holosensor, spectroscopic holographic 3D imaging of outdoor 3D scenes will be realized without mechanically moving parts.

We have reviewed progress on IDH with an image sensor and its applications to microscopy and compact hologram recorders. Improvements of specifications such as measurement speed, image quality, and further downsizing are important next steps in IDH. Dynamic range, sensitivity, and low noise of an image sensor are now particularly important to obtain an incoherent digital hologram because the visibility and light intensity of such a hologram are lower than those of a hologram generated with a laser. Its importance on advanced digital signal processing techniques based on informatics such as deep learning and compressive sensing will also be increased (Wu et al., 2020; Wu et al., 2021). Algorithms for accelerating holographic image reconstruction are continuously developed and these will lead to real-time holographic measurement (Tsuruta et al., 2021; Shimobaba et al., 2022). Applications to the development of multidimensional imaging and measurement apparatus will be realized with the advancements in state-of-the-art optics, photonics, optical devices, and information science.

AUTHOR CONTRIBUTIONS

The author has written the review article. The experimental results shown in this review article were obtained with the co-authors of the related papers.

FUNDING

This study is partially supported by The Mitsubishi Foundation (No. 202111007), Japan Science and Technology Agency (JST) Precursory Research for Embryonic Science and Technology (PRESTO) (JPMJPR16P8), Japan Society for the Promotion of Science (JSPS) (JP18H01456), and Cooperative Research Program of "Network Joint Research Center for Materials and Devices" (No. 20211086).

ACKNOWLEDGMENTS

TT sincerely thank co-workers and co-authors of the research studies related to this review.

REFERENCES

Awatsuji, Y., Sasada, M., and Kubota, T. (2004). Parallel Quasi-Phase-Shifting Digital Holography. *Appl. Phys. Lett.* 85, 1069–1071. doi:10.1063/1.1777996

Brooker, G., Siegel, N., Wang, V., and Rosen, J. (2011). Optimal Resolution in Fresnel Incoherent Correlation Holographic Fluorescence Microscopy. *Opt. Express* 19, 5047–5062. doi:10.1364/oe.19.005047

Bruning, J. H., Herriott, D. R., Gallagher, J. E., Rosenfeld, D. P., White, A. D., and Brangaccio, D. J. (1974). Digital Wavefront Measuring Interferometer for

- Testing Optical Surfaces and Lenses. *Appl. Opt.* 13, 2693–2703. doi:10.1364/ao.13.002693
- Choi, K., Yim, J., and Min, S.-W. (2018). Achromatic Phase Shifting Self-Interference Incoherent Digital Holography Using Linear Polarizer and Geometric Phase Lens. *Opt. Express* 26, 16212–16225. doi:10.1364/oe.26.016212
- Choi, K., Joo, K.-I., Lee, T.-H., Kim, H.-R., Yim, J., Do, H., et al. (2019). Compact Self-Interference Incoherent Digital Holographic Camera System with Real-Time Operation. *Opt. Express* 27, 4818–4833. doi:10.1364/oe.27.004818
- Clark, D. C., and Kim, M. K. (2015). Nonscanning Three-Dimensional Differential Holographic Fluorescence Microscopy. *J. Electron. Imaging* 24, 043014. doi:10.1117/1.jei.24.4.043014
- Hara, T., Tahara, T., Ichihashi, Y., Oi, R., and Ito, T. (2020). Multiwavelength-multiplexed Phase-Shifting Incoherent Color Digital Holography. *Opt. Express* 28, 10078–10089. doi:10.1364/oe.383692
- Hong, J., and Kim, M. K. (2013). Single-shot Self-Interference Incoherent Digital Holography Using off-axis Configuration. *Opt. Lett.* 38, 5196–5199. doi:10.1364/ol.38.005196
- Imbe, M. (2019). Radiometric Temperature Measurement by Incoherent Digital Holography. *Appl. Opt.* 58, A82–A89. doi:10.1364/ao.58.000a82
- Jang, C., Kim, J., Clark, D. C., Lee, S., Lee, B., and Kim, M. K. (2015). Holographic Fluorescence Microscopy with Incoherent Digital Holographic Adaptive Optics. *J. Biomed. Opt.* 20, 111204. doi:10.1117/1.jbo.20.11.111204
- Kalenkov, S. G., Kalenkov, G. S., and Shtanko, A. E. (2019). Self-reference Hyperspectral Holographic Microscopy. *J. Opt. Soc. Am. A* 36, A34–A38. doi:10.1364/josaa.36.000a34
- Kelner, R., and Rosen, J. (2012). Spatially Incoherent Single Channel Digital Fourier Holography. *Opt. Lett.* 37, 3723–3725. doi:10.1364/ol.37.003723
- Kim, M. K. (2012). Adaptive Optics by Incoherent Digital Holography. *Opt. Lett.* 37, 2694–2696. doi:10.1364/ol.37.002694
- Kim, M. K. (2013). Full Color Natural Light Holographic Camera. *Opt. Express* 21, 9636–9642. doi:10.1364/oe.21.009636
- Kumar, M., Quan, X., Awatsuji, Y., Cheng, C., Hasebe, M., Tamada, Y., et al. (2020). Common-path Multimodal Three-Dimensional Fluorescence and Phase Imaging System. *J. Biomed. Opt.* 25, 1–15. doi:10.1117/1.JBO.25.3.032010
- Liang, D., Zhang, Q., Wang, J., and Liu, J. (2020). Single-shot Fresnel Incoherent Digital Holography Based on Geometric Phase Lens. *J. Mod. Opt.* 67, 92–98. doi:10.1080/09500340.2019.1695970
- Liebel, M., Pazos-Perez, N., van Hulst, N. F., and Alvarez-Puebla, R. A. (2020). Surface-enhanced Raman Scattering Holography. *Nat. Nanotechnol.* 15, 1005–1011. doi:10.1038/s41565-020-0771-9
- Liebel, M., Ortega Arroyo, J., Beltrán, V. S., Osmond, J., Jo, A., Lee, H., et al. (2020). 3D Tracking of Extracellular Vesicles by Holographic Fluorescence Imaging. *Sci. Adv.* 6, eabc2508. doi:10.1126/sciadv.abc2508
- Liu, J.-P., Tahara, T., Hayasaki, Y., and Poon, T.-C. (2018). Incoherent Digital Holography: a Review. *Appl. Sci.* 8, 143. doi:10.3390/app8010143
- Lohmann, A., and Bryngdahl, O. (1968). One-dimensional Holography with Spatially Incoherent Light. *J. Opt. Soc. Am.* 58, 625–628.
- Lohmann, A. W. (1965). Wavefront Reconstruction for Incoherent Objects. *J. Opt. Soc. Am.* 55, 1555–1556. doi:10.1364/josa.55.1555_1
- Marar, A., and Kner, P. (2020). Three-dimensional Nanoscale Localization of point-like Objects Using Self-Interference Digital Holography. *Opt. Lett.* 45, 591–594. doi:10.1364/ol.379047
- Millerd, J., Brock, N., Hayes, J., Morris, M. N., Novak, M., and Wyant, J. (2004). Pixelated Phase-Mask Dynamic Interferometer. *Proc. SPIE* 5531, 304–314. doi:10.1117/12.560807
- Mugnier, L. M., and Sirat, G. Y. (1992). On-axis Conoscopic Holography without a Conjugate Image. *Opt. Lett.* 17, 294–296. doi:10.1364/ol.17.000294
- Mugnier, L. M., Sirat, G. Y., and Charlot, D. (1993). Conoscopic Holography: Two-Dimensional Numerical Reconstructions. *Opt. Lett.* 18, 66–68. doi:10.1364/ol.18.000066
- Mugnier, L. M. (1995). Conoscopic Holography: toward Three-Dimensional Reconstructions of Opaque Objects. *Appl. Opt.* 34, 1363–1371. doi:10.1364/ao.34.001363
- Naik, D. N., Ezawa, T., Miyamoto, Y., and Takeda, M. (2009). 3-D Coherence Holography Using a Modified Sagnac Radial Shearing Interferometer with Geometric Phase Shift. *Opt. Express* 17, 10633–10641. doi:10.1364/oe.17.010633
- Naik, D. N., Pedrini, G., Takeda, M., and Osten, W. (2014). Spectrally Resolved Incoherent Holography: 3D Spatial and Spectral Imaging Using a Mach-Zehnder Radial-Shearing Interferometer. *Opt. Lett.* 39, 1857–1860. doi:10.1364/ol.39.001857
- Nobukawa, T., Muroi, T., Katano, Y., Kinoshita, N., and Ishii, N. (2018). Single-shot Phase-Shifting Incoherent Digital Holography with Multiplexed Checkerboard Phase Gratings. *Opt. Lett.* 43, 1698–1701. doi:10.1364/ol.43.001698
- Nobukawa, T., Katano, Y., Muroi, T., Kinoshita, N., and Ishii, N. (2019). Bimodal Incoherent Digital Holography for Both Three-Dimensional Imaging and Quasi-Infinite-Depth-Of-Field Imaging. *Sci. Rep.* 9, 3363. doi:10.1038/s41598-019-39728-8
- Okamoto, R., and Tahara, T. (2021). Precision Limit for Simultaneous Phase and Transmittance Estimation with Phase-Shifting Interferometry. *Phys. Rev. A* 104, 033521. doi:10.1103/physreva.104.033521
- Pedrini, G., Li, H., Faridian, A., and Osten, W. (2012). Digital Holography of Self-Luminous Objects by Using a Mach-Zehnder Setup. *Opt. Lett.* 37, 713–715. doi:10.1364/ol.37.000713
- Poon, T. C., and Korpel, A. (1979). Optical Transfer Function of an Acousto-Optic Heterodyning Image Processor. *Opt. Lett.* 4, 317–319. doi:10.1364/ol.4.000317
- Poon, T.-C. (1985). Method of Two-Dimensional Bipolar Incoherent Image Processing by Acousto-Optic Two-Pupil Synthesis. *Opt. Lett.* 10, 197–199. doi:10.1364/ol.10.000197
- Poon, T.-C. (2007). *Optical Scanning Holography with MATLAB*. New York: Springer.
- Poon, T.-C. (2009). Optical Scanning Holography - A Review of Recent Progress. *J. Opt. Soc. Korea* 13, 406–415. doi:10.3807/josk.2009.13.4.406
- Potcoava, M., Mann, C., Art, J., and Alford, S. (2021). Spatio-temporal Performance in an Incoherent Holography Lattice Light-Sheet Microscope (IHLLS). *Opt. Express* 29, 23888–23901. doi:10.1364/OE.425069
- Quan, X., Matoba, O., and Awatsuji, Y. (2017). Single-shot Incoherent Digital Holography Using a Dual-Focusing Lens with Diffraction Gratings. *Opt. Lett.* 42, 383–386. doi:10.1364/ol.42.000383
- Rosen, J., and Brooker, G. (2007). Digital Spatially Incoherent Fresnel Holography. *Opt. Lett.* 32, 912–914. doi:10.1364/ol.32.000912
- Rosen, J., and Brooker, G. (2008). Non-scanning Motionless Fluorescence Three-Dimensional Holographic Microscopy. *Nat. Photon* 2, 190–195. doi:10.1038/nphoton.2007.300
- Rosen, J., Siegel, N., and Brooker, G. (2011). Theoretical and Experimental Demonstration of Resolution beyond the Rayleigh Limit by FINCH Fluorescence Microscopic Imaging. *Opt. Express* 19, 26249–26268. doi:10.1364/oe.19.026249
- Rosen, J., Vijayakumar, A., Kumar, M., Rai, M. R., Kelner, R., Kashter, Y., et al. (2019). Recent Advances in Self-Interference Incoherent Digital Holography. *Adv. Opt. Photon.* 11, 1–66. doi:10.1364/aop.11.000001
- Rosen, J., Alford, S., Anand, V., Art, J., Bouchal, P., Bouchal, Z., et al. (2021). Roadmap on Recent Progress in FINCH Technology. *J. Imaging* 7, 197. doi:10.3390/jimaging7100197
- Sato, T., Araki, T., Sasaki, Y., Tsuru, T., Tadokoro, T., and Kawakami, S. (2007). Compact Ellipsometer Employing a Static Polarimeter Module with Arrayed Polarizer and Wave-Plate Elements. *Appl. Opt.* 46, 4963–4967. doi:10.1364/ao.46.004963
- Schilling, B. W., Poon, T.-C., Indebetouw, G., Storrie, B., Shinoda, K., Suzuki, Y., et al. (1997). Three-dimensional Holographic Fluorescence Microscopy. *Opt. Lett.* 22, 1506–1508. doi:10.1364/ol.22.001506
- Shimobaba, T., Tahara, T., Hoshi, I., Shiomi, H., Wang, F., Hara, T., et al. (2022). Real-valued Diffraction Calculations for Computational Holography [Invited]. *Appl. Opt.* 61, B96–B102. doi:10.1364/ao.443439
- Sirat, G., and Psaltis, D. (1985). Conoscopic Holography. *Opt. Lett.* 10, 4–6. doi:10.1364/ol.10.000004
- Tahara, T., and Oi, R. (2021). Palm-sized Single-Shot Phase-Shifting Incoherent Digital Holography System. *OSA Continuum* 4, 2372–2380. doi:10.1364/osac.431930
- Tahara, T., and Sato, I. (2019). “Single-shot Color Digital Holographic Microscopy with white Light,” in Proceedings of 3D Image Conf. 2019, in Japanese, 4–1.
- Tahara, T., Mori, R., Kikunaga, S., Arai, Y., and Takaki, Y. (2015). Dual-wavelength Phase-Shifting Digital Holography Selectively Extracting Wavelength

- Information from Wavelength-Multiplexed Holograms. *Opt. Lett.* 40, 2810–2813. doi:10.1364/ol.40.002810
- Tahara, T., Mori, R., Arai, Y., and Takaki, Y. (2015). Four-step Phase-Shifting Digital Holography Simultaneously Sensing Dual-Wavelength Information Using a Monochromatic Image Sensor. *J. Opt.* 17, 125707–126110. doi:10.1088/2040-8978/17/12/125707
- Tahara, T., Kanno, T., Arai, Y., and Ozawa, T. (2017). Single-shot Phase-Shifting Incoherent Digital Holography. *J. Opt.* 19, 065705. doi:10.1088/2040-8986/aa6e82
- Tahara, T., Otani, R., Omae, K., Gotohda, T., Arai, Y., and Takaki, Y. (2017). Multiwavelength Digital Holography with Wavelength-Multiplexed Holograms and Arbitrary Symmetric Phase Shifts. *Opt. Express* 25, 11157–11172. doi:10.1364/oe.25.011157
- Tahara, T., Kikunaga, S., and Arai, Y. (2018). *Digital Holography Apparatus and Digital Holography Method*. Japanese patent No. JP6308594.
- Tahara, T., Quan, X., Otani, R., Takaki, Y., and Matoba, O. (2018). Digital Holography and its Multidimensional Imaging Applications: a Review. *Microscopy* 67, 55–67. doi:10.1093/jmicro/dfy007
- Tahara, T., Hara, T., Ichihashi, Y., Oi, R., and Ito, T. (2019). “Simultaneous Holographic Multicolor Sensing of Multiple Natural Light Sources Based on Computational Coherent Superposition,” in *Proceedings of Optics and Photonics Japan 2019 (OPJ)* (in Japanese: Optical Society of Japan OSJ), PDP6.
- Tahara, T., Ito, T., Ichihashi, Y., and Oi, R. (2020). “Single-shot Incoherent Digital Holographic Microscopy System without a Spatial Light Modulator,” in *Digital Holography and Three-Dimensional Imaging 2020 (DH)*, OSA Technical Digest (Optical Society of America). HF3D.5.
- Tahara, T., Ito, T., Ichihashi, Y., and Oi, R. (2020). Single-shot Incoherent Color Digital Holographic Microscopy System with Static Polarization-Sensitive Optical Elements. *J. Opt.* 22, 105702. doi:10.1088/2040-8986/abb007
- Tahara, T., Ito, T., Ichihashi, Y., and Oi, R. (2020). Multiwavelength Three-Dimensional Microscopy with Spatially Incoherent Light, Based on Computational Coherent Superposition. *Opt. Lett.* 45, 2482–2485. doi:10.1364/ol.386264
- Tahara, T., Ishii, A., Ito, T., Ichihashi, Y., and Oi, R. (2020). Single-shot Wavelength-Multiplexed Digital Holography for 3D Fluorescent Microscopy and Other Imaging Modalities. *Appl. Phys. Lett.* 117, 031102. doi:10.1063/5.0011075
- Tahara, T., Koujin, T., Matsuda, A., Ishii, A., Ito, T., Ichihashi, Y., et al. (2021). Incoherent Color Digital Holography with Computational Coherent Superposition for Fluorescence Imaging [Invited]. *Appl. Opt.* 60, A260–A267. doi:10.1364/ao.406068
- Tahara, T., Kozawa, Y., Ishii, A., Wakunami, K., Ichihashi, Y., and Oi, R. (2021). Two-step Phase-Shifting Interferometry for Self-Interference Digital Holography. *Opt. Lett.* 46, 669–672. doi:10.1364/ol.414083
- Tahara, T., Kozawa, Y., Koujin, T., Matsuda, A., and Oi, R. (2021). Incoherent Digital Holographic Microscopy for High-Speed Three-Dimensional Motion-Picture Sensing. *Proc. SPIE* 11898, 118980D. doi:10.1117/12.2599725
- Tahara, T., Kozawa, Y., Matsuda, A., and Oi, R. (2021). Quantitative Phase Imaging with Single-Path Phase-Shifting Digital Holography Using a Light-Emitting Diode. *OSA Continuum* 4, 2918–2927. doi:10.1364/osac.435949
- Tahara, T., Koujin, T., Matsuda, A., Kozawa, Y., and Oi, R. (2021e). “72 Fps Incoherent Two-Color Digital Motion-Picture Holography System for Fluorescence Cell Imaging,” in *Digital Holography and Three-Dimensional Imaging 2021 (DH)*, OSA Technical Digest (Optical Society of America). DTu6H.5. doi:10.1364/dh.2021.dtu6h.5
- Tahara, T., Okamoto, R., Ishii, A., Kozawa, Y., Koujin, T., Matsuda, A., et al. (2021f). Phase-shifting Interferometry for Multidimensional Incoherent Digital Holography and toward Ultimately Low Light Sensing. *Proc. SPIE*, 1205752. doi:10.1117/12.2607197
- Tahara, T., Kozawa, Y., and Oi, R. (2022). Single-path Single-Shot Phase-Shifting Digital Holographic Microscopy without a Laser Light Source. *Opt. Express* 30, (in press). 1182–1194. doi:10.1364/OE.442661
- Tahara, T. (2021). Discussions and Visions for Multidimension-Multiplexed Incoherent Digital Motion-Picture Holography. *Rev. Laser Eng.* 49, 321–324.
- Takeda, M., Wang, W., Duan, Z., and Miyamoto, Y. (2005). Coherence Holography. *Opt. Express* 13, 9629–9635. doi:10.1364/ope.13.009629
- Tankam, P., Picart, P., Mounier, D., Desse, J. M., and Li, J.-C. (2010). Method of Digital Holographic Recording and Reconstruction Using a Stacked Color Image Sensor. *Appl. Opt.* 49, 320–328. doi:10.1364/ao.49.000320
- Teeranunranont, S., and Yoshimori, K. (2013). Digital Holographic Three-Dimensional Imaging Spectrometry. *Appl. Opt.* 52, A388–A396. doi:10.1364/ao.52.00a388
- Ting-Chung Poon, T. C., Ming Hsien Wu, M. H., Shinoda, K., and Suzuki, Y. (1996). Optical Scanning Holography. *Proc. IEEE* 84, 753–764. doi:10.1109/5.488744
- Tsuruta, M., Fukuyama, T., Tahara, T., and Takaki, Y. (2021). Fast Image Reconstruction Technique for Parallel Phase-Shifting Digital Holography. *Appl. Sci.* 11, 11343. doi:10.3390/app112311343
- Ueda, K., and Takuma, H. (1984). A Novel Spectrometric Technique Based on Fourier Transformation of Transmission Signal of Faraday Rotator. *Rev. Laser Eng.* 12, 41. (in Japanese). doi:10.2184/ljs.12.652
- Vijayakumar, A., and Rosen, J. (2017). Spectrum and Space Resolved 4D Imaging by Coded Aperture Correlation Holography (COACH) with Diffractive Objective Lens. *Opt. Lett.* 42, 947–950. doi:10.1364/ol.42.000947
- Vijayakumar, A., Kashter, Y., Kelner, R., and Rosen, J. (2016). Coded Aperture Correlation Holography-A New Type of Incoherent Digital Holograms. *Opt. Express* 24, 12430–12441. doi:10.1364/oe.24.012430
- Wu, J., Zhang, H., Zhang, W., Jin, G., Cao, L., and Barbastathis, G. (2020). Single-shot Lensless Imaging with Fresnel Zone Aperture and Incoherent Illumination. *Light Sci. Appl.* 9, 53. doi:10.1038/s41377-020-0289-9
- Wu, J., Cao, L., and Barbastathis, G. (2021). DNN-FZA Camera: a Deep Learning Approach toward Broadband FZA Lensless Imaging. *Opt. Lett.* 46, 130–133. doi:10.1364/ol.411228
- Yamaguchi, I., and Zhang, T. (1997). Phase-shifting Digital Holography. *Opt. Lett.* 22, 1268–1270. doi:10.1364/ol.22.001268
- Yanagawa, T., Abe, R., and Hayasaki, Y. (2015). Three-dimensional Mapping of Fluorescent Nanoparticles Using Incoherent Digital Holography. *Opt. Lett.* 40, 3312–3315. doi:10.1364/ol.40.003312
- Yoneda, N., Saita, Y., and Nomura, T. (2021). Three-dimensional Fluorescence Imaging through Dynamic Scattering media by Motionless Optical Scanning Holography. *Appl. Phys. Lett.* 119, 161101. doi:10.1063/5.0066358
- Yoshimori, K. (2001). Interferometric Spectral Imaging for Three-Dimensional Objects Illuminated by a Natural Light Source. *J. Opt. Soc. Am. A*. 18, 765–770. doi:10.1364/josaa.18.000765
- Zhu, B., and Ueda, K.-i. (2003). Real-time Wavefront Measurement Based on Diffraction Grating Holography. *Opt. Commun.* 225, 1–6. doi:10.1016/j.optcom.2003.07.025

Conflict of Interest: The author declares that the research was conducted in the absence of any commercial or financial relationships that could be construed as a potential conflict of interest.

Publisher’s Note: All claims expressed in this article are solely those of the authors and do not necessarily represent those of their affiliated organizations, or those of the publisher, the editors and the reviewers. Any product that may be evaluated in this article, or claim that may be made by its manufacturer, is not guaranteed or endorsed by the publisher.

Copyright © 2022 Tahara. This is an open-access article distributed under the terms of the Creative Commons Attribution License (CC BY). The use, distribution or reproduction in other forums is permitted, provided the original author(s) and the copyright owner(s) are credited and that the original publication in this journal is cited, in accordance with accepted academic practice. No use, distribution or reproduction is permitted which does not comply with these terms.